

A METHOD TO DETECT STRUCTURAL DAMAGE USING HIGH-FREQUENCY SEISMOGRAMS

Vanessa M. Heckman¹⁾, Monica D. Kohler²⁾, and Thomas H. Heaton³⁾

1) Graduate Student, Department of Mechanical and Civil Engineering, California Institute of Technology, USA

2) Professional Researcher, Center for Embedded Networked Sensing, University of California at Los Angeles, USA

*3) Professor of Engineering Seismology, Department of Mechanical and Civil Engineering, California Institute of Technology, USA
heckman@caltech.edu, kohler@ess.ucla.edu, heaton@caltech.edu*

Abstract: A numerical study is performed to gain insight into applying a novel method to detect high-frequency dynamic failure in buildings. The method relies on prerecorded catalog of Green's functions for instrumented buildings. Structural failure during a seismic event is detected by screening continuous data for the presence of waveform similarities to each of the cataloged building responses. In the first part of this numerical study, an impulse-like force is applied to a beam column connection in a linear elastic steel frame. A time-reversed reciprocal method is used to demonstrate that the resulting simulated displacements can be used to determine the absolute time and location of the applied force. In the second part of the study, a steel frame's response to two loading cases, an impulse-like force and an opening crack tensile stress, is computed on a temporal scale of microseconds. Results indicate that the velocity waveform generated by a tensile crack can be approximated by the velocity waveform generated by an impulse-like force load applied at the proper location. These results support the idea of using a nondestructive impulse-like force (e.g. hammer blow) to characterize the building response to high-frequency dynamic failure (e.g. weld fracture).

1. INTRODUCTION

There has been recent interest in using acoustic techniques to detect damage in instrumented civil structures. An automated damage detection method that analyzes recorded data has application to building types that are susceptible to a signature type of failure, where locations of potential structural damage are known a priori. Such a method would be valuable if it could be used to detect types of damage that are otherwise difficult and costly to detect. In particular, this method has application to the detection of brittle failure of welded beam-column connections in steel moment resisting frames (MRFs). The 1994 Northridge earthquake exposed this type of damage, which can occur without accompanying damage to architectural finishes and cladding; in some cases, detection requires intrusive inspections that can be costly and time-consuming (Rodgers et al. 2007). An automated damage detection method could be used to located areas of probable damage to guide post-earthquake building inspection.

Acoustic damage detection methods rely on the comparison of a recent signal to an archived baseline response function, known as a template. The template is recorded at a time when the structure is undamaged. The sensor network must have a high sampling rate to capture the propagation of waves throughout the structure. Acoustic techniques have been explored experimentally and numerically for thin plates and beams (Park et al. 2007,

Wang and Rose 2003, Wang et al. 2004), which serve as waveguides that effectively carry information from the location of structural damage to a receiver. This information, namely differences in waveform and amplitude between the current signal and the template, are used to diagnose damage.

Acoustic methods can be passive or active, and sensor networks can be permanently installed or temporary. Giurgiutiu (2005) reviews current techniques, including embedded ultrasonic non-destructive evaluation (NDE), which uses a transmitter to interrogate the structure while a receiver records the structural response.

1) *Pitch-catch*: A pulse is emitted by a transmitter and travels through the material to a receiver. Differences in guided wave shape, phase, and amplitude are used to detect damage in the medium between the transmitter and receiver.

2) *Pulse-echo*: A pulse is emitted by a transmitter, which also acts as a receiver to detect damage in the form of additional echoes.

3) *Time-reversal*: A signal sent by a transmitter arrives at a receiver, where the signal is time-reversed and reemitted. Structural damage that causes linear reciprocity to break down leads to discrepancy between the original signal and the final signal received by the transmitter.

4) *Migration*: Recorded waves are back-propagated through the material by systematically solving the wave equation to image reflectors in the medium.

In this paper, a complementary acoustic method is

presented, that makes use of a prerecorded catalog of Green's functions and a matched filter method to passively detect the original failure event. This technique is different from existing acoustic methods as it is designed to recognize seismic waves radiated by the original brittle failure event. The matched filter method has been successfully used in other fields (Gibbons and Ringdal 2006, Anstey 1964), but the method has yet to be explored in the context of acoustic damage detection of civil structures.

The proposed method is described in greater detail in the following section. Two numerical studies are performed; the first compares our method to a similar time-reversed reciprocal method, and the second provides a waveform comparison between a non-destructive event and a failure event.

2. MATCHED FILTER METHOD

The proposed method would make use of a prerecorded catalog of Green's functions for an instrumented building to detect structural damage during a later seismic event. Continuous data collected on a passive network is screened for the presence of waveform similarity to one of the Green's function templates. The method is outlined below.

- 1) Identify probable points of failure in an instrumented building before structural damage has occurred. As pre-Northridge steel MRFs are susceptible to the brittle failure of welded beam-column connections, these would be the locations of probable failure for this type of building.
- 2) At each labeled location, apply a short-duration high-frequency pulse (e.g. using a force transducer hammer). The response of the building at each instrument site is the Green's function specific to that source location-receiver pair. The Green's functions are archived in the catalog of templates to be used later to screen the high-frequency seismogram for a damage signal.
- 3) For each possible source location k , perform a running cross-correlation between the Green's function templates for that source location and a moving window of the seismogram that recorded the shaking event, stacking over the receivers. Cross-correlation between the k^{th} Green's function template x_i^k recorded by the i^{th} receiver and the seismogram x_i recorded by the i^{th} receiver is given by

$$C_i^k(t) = \frac{\int_0^T x_i^k(\tau) x_i(t + \tau) d\tau}{\left(\int_0^T (x_i^k(\tau))^2 d\tau \int_0^T (x_i(t + \tau))^2 d\tau \right)^{1/2}} \quad (1)$$

Time T is the duration of the template, and the cross-correlation is normalized by the autocorrelation values for the given time window.

Compute the stacked cross-correlation function by summing over the R receiver locations to obtain

$$C^k(t) = \frac{1}{R} \sum_{i=1}^R C_i^k(t). \quad (2)$$

- 4) If damage occurred at or near the k^{th} source location, the stacked cross-correlation function given by Eq. (2) should peak at a value close to one at the correct time of the structural damage event. In the case of multiple locations of damage, then the stacked cross-correlation functions should each peak at a value close to one at the corresponding times, provided the correct Green's function templates are used. This procedure could be extended to the three-dimensional case.

The proposed method makes some assumptions. The first is that the signal due to the failure event will be observable over the predominant building response to seismic loading. Rodgers et al. (2007) carried out experimentation on a one-third scale model steel moment frame and found that "high-frequency high-amplitude transient accelerations" were observable over the structural response to shaking and could be attributed to connection fracture. They further analyzed building records from the 1994 Northridge earthquake by identifying transient signals and classifying the possible causes, and they were able to determine with a 67% success rate whether each building had undergone connection fracture.

A second assumption is that the template will not change significantly over time. However, it has been shown that changes in environmental conditions as well as moderately large local earthquakes can lead to observed changes in a building's natural frequency (Clinton et al. 2006). This has not been extended to observed changes in wave propagation through the structural components of the building. A similar matched filter method has been successfully employed by Gibbons and Ringdal (2006) to detect similar low-magnitude seismic events by cross-correlating a waveform template with successive time segments of incoming data and stacking over the seismic array.

A third assumption is that the sensor network will be able to capture waves propagating away from the damage location throughout the structure. Kohler et al. (2009) have carried out preliminary experimentation on the UCLA Factor building using hammer blows to generate Green's function templates. The structural response to the hammer blow was observable well above ambient noise, and the signal could be seen to propagate away from the source location at a downsampled rate of 200 sps, achieved by filtering the 500 sps accelerometer array data for frequencies between 10 and 95 Hz.

A fourth assumption is that the Green's function template will be similar to the damage signal. This assumption is addressed in Section 4.

3. A TIME-REVERSED RECIPROCAL NUMERICAL EXPERIMENT

A time-reversed reciprocal method is applied to demonstrate that the location of a nondestructive

impulse-like force can be determined by using the numerically computed displacement records to time-reverse and retransmit the signal. First, the response of a two-story one-bay steel frame to an impulse-like force applied to a beam-column connection is computed. A cross section of the three-dimensional steel model is shown in Figure 1 below. Each beam and column has a square cross section of length 0.5 m. The model parameters are governed by linear elastic material properties of A36 structural steel ($E = 200$ GPa, $\mu = 80$ GPa, $\rho = 7850$ kg/m³), which correspond to seismic velocities of $c_s = 3.2$ km/s and $c_p = 5.6$ km/s. The hex 8 mesh elements have a discretization length of 2.5 cm; the total time is 4 ms with a time step of 2 μ s. CUBIT is used for mesh generation, PyLith for physics code, and ParaView for visualization (Aagaard 2008).

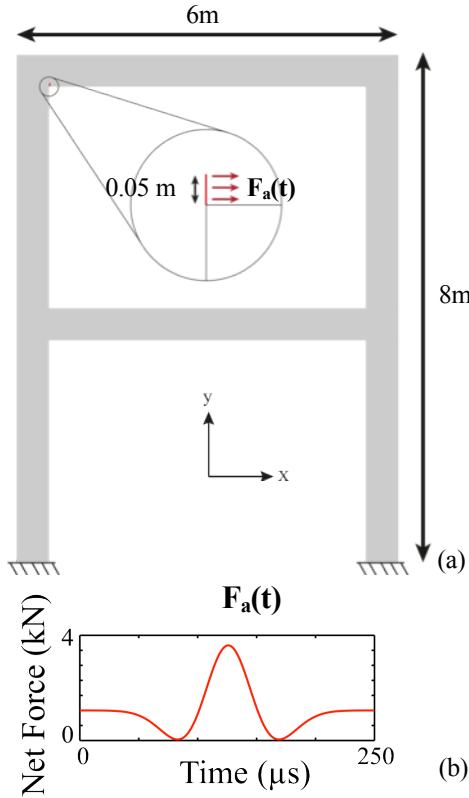


Figure 1 Numerical Setup for Steel Frame: (a) Impulse-like force is applied at beam-column connection in a direction parallel to the x-axis (b) Ricker wavelet is used for time-force history.

3.1 Forward Simulation

The response of the steel frame to an impulse-like force applied to a beam-column connection is computed. As shown in Figure 1 above, the force is applied along the positive x-axis to the close-up section of the connection. The total force is distributed proportionally over nodes according to the amount of surface area contained by each node. The force-time history is a Ricker wavelet.

Waves propagate away from the location of the source, reflecting off the edges of the frame, as shown in Figure 2 below. Resulting displacements are recorded at the twelve receiver locations approximately evenly spaced along the

central cross section of the frame. A representative sample of displacements is provided in Figure 3(a) below.

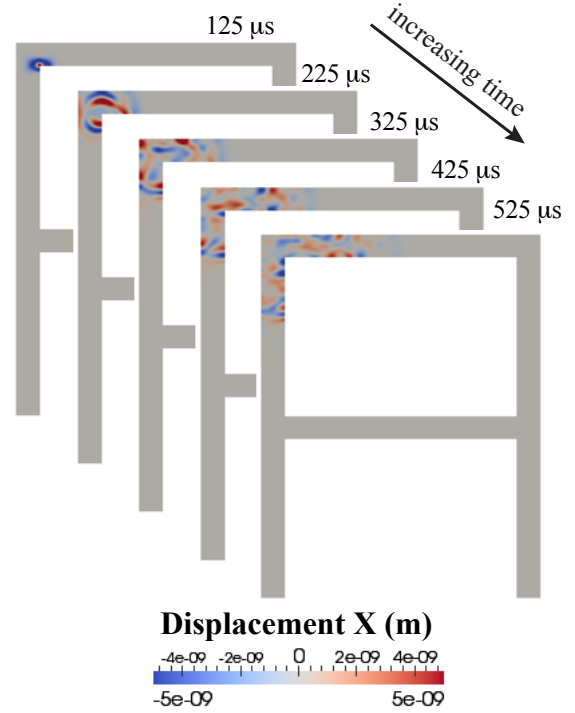


Figure 2 Response of Steel Frame to Nondestructive Impulse-like Force Applied to Beam-Column Connection.

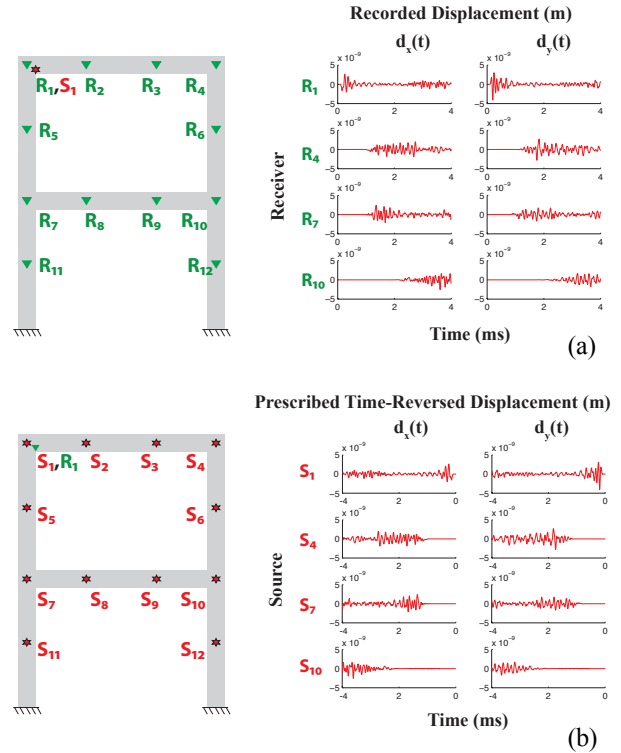


Figure 3 Receivers, Sources, and Displacements: (a) Receiver locations and examples of recorded displacements for forward simulation. (b) Source locations and corresponding prescribed time-reverse displacements for reverse simulation. Due to symmetry, $d_z(t) = 0$.

3.2 Reverse Simulation

Following the time-reversed reciprocal method, the receiver and source locations are interchanged, and each of the displacement records is time-reversed and applied at the respective new source location as prescribed Dirichlet conditions, as shown in Figure 3(b) above. The retransmitted signal propagates through the frame, and the waves generated by the twelve new source locations interfere constructively to focus at the original source location S_1 , where the nondestructive load was applied, and at the correct time. To simplify timing, the reverse simulation begins at -4 ms and ends at 0 ms, with waves focusing on the beam-column connection at the correct time of -125 μ s, demonstrated in Figure 4 below. Thus, by using a time-reversed reciprocal method, the recorded displacements are used to determine the absolute time and location of the original applied force.

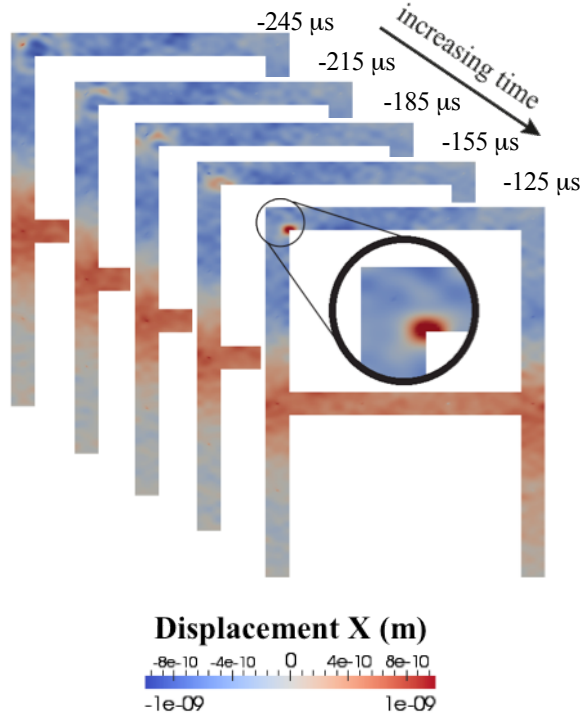


Figure 4 Response of Steel Frame to Prescribed Time-Reversed Displacements. Waves generated at each of the twelve source locations converge at the correct location at the correct time.

4. NUMERICAL APPLICATION OF MATCHED FILTER METHOD

A time-reversed reciprocal method as presented in the previous section is not application-realistic, as the location of the receiver may not coincide with the location of damage, and thus, the focusing of the transmitted time-reversed signal could go undetected. The purpose of this section is to investigate numerically an alternative yet similar approach that makes use of Green's functions, waveform similarity,

and wave propagation reciprocity. The matched filter method is used to screen data recorded by a passive seismic network for waveform similarities to an archived template, ultimately relying on experimental, not simulated, building response. To validate the feasibility of the proposed method, it is first necessary to provide justification for using the structural response to an impulse-like force to approximate the structural response to an opening crack tensile stress.

4.1 Comparison of Structural Response to Two Different Source Conditions

The response of a steel frame to two different loading cases, an impulse-like force and an opening crack tensile stress, both shown in Figure 5, is compared to determine whether the waveform generated by a nondestructive source can be used to approximate the waveform generated by a structurally damaging source. The same material properties and dimensions as in Section 3 are used. A square notch is introduced in the opening crack tensile stress case, to simulate crack initiation at the beam-column connection. The square notch has a length of 0.05 m, consistent with the dimensions used for the unnotched frame.

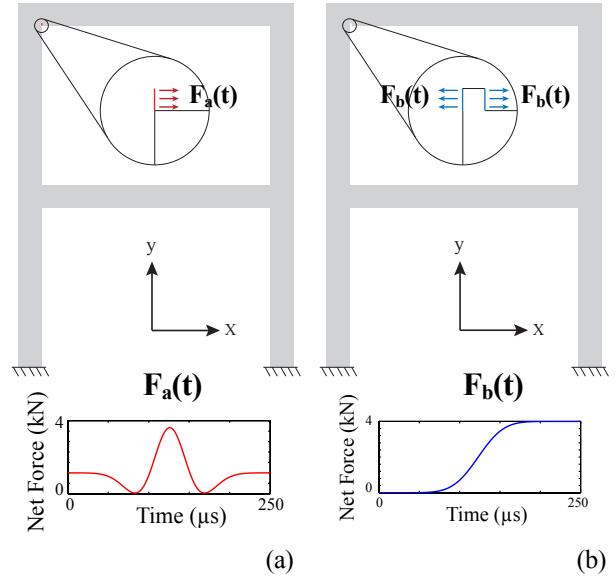


Figure 5 Numerical Setup: (a) Impulse-like force using Ricker wavelet force-time history applied to top left beam-column connection in an unnotched frame, and (b) Opening crack tensile stress using error function force-time history applied to the same connection in a notched frame.

Resulting displacements and velocities are recorded at four receivers located along the central cross section of the frame, shown in Figure 6 below. The simulation is repeated at each of the four source locations for both a force impulse and a tensile crack.

The displacement records, provided in Figure 7 below, generated by using the nondestructive source differ significantly between the displacement records generated by using the structurally damaging sources, primarily due to the static offset across the notch. The two sets of velocity

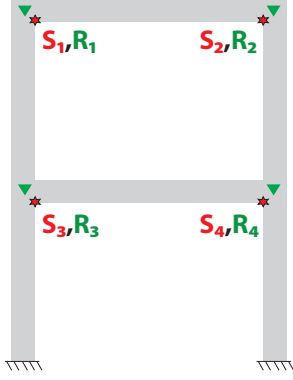


Figure 6 Source and Receiver Locations.

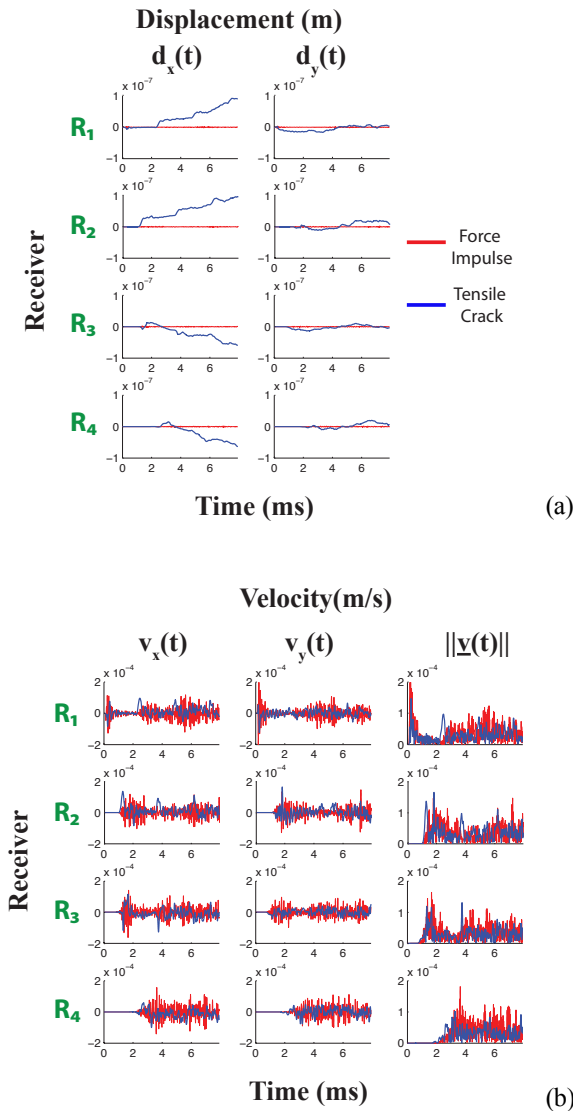


Figure 7 High-Frequency Seismograms Using Source Location S_1 : (a) Displacements differ significantly between the impulse-like force (red) and opening crack tensile stress (blue) case. (b) Velocities provide a better agreement, and polarity differences are improved by taking the absolute value or magnitude of the record. Due to symmetry, $d_z=v_z=0$.

records are more similar to each other than are the two sets of displacement records. The similarities between force impulse and tensile crack velocity waveforms underscore the fact that, for traveling elastic waves, the strains are proportional to their associated particle velocities, regardless of the source mechanism. Thus, the template is created using the velocity record.

4.2 Stacked Cross-Correlation Values

A stacked cross-correlation method is used to determine the similarity of velocity waveforms generated by a force impulse at source location S_k and a tensile crack at source location S_l . The summarized method follows:

1) A set of velocities $\{v_1^k(t), v_2^k(t), v_3^k(t), v_4^k(t)\}$ are recorded for a force impulse applied at source location S_k , where $v_i^k(t)$ is the three-component velocity vector recorded at the i^{th} receiver. Due to symmetry and the fact that the receivers are located along the central cross section of the frame, the z -component of the velocity vector is zero.

2) The set of envelopes $\{e_1^k(t), e_2^k(t), e_3^k(t), e_4^k(t)\}$ is computed using the velocities. The magnitude of each 3-component envelope is passed through a low-pass filter to produce a set of scalar functions of time $\{e_1^k(t), e_2^k(t), e_3^k(t), e_4^k(t)\}$. These records are archived as our template signals for damage caused at the k^{th} source location. The duration of our template is time T .

3) Similarly, a set of scalar filtered envelopes for a tensile crack at the l^{th} source location S_l are computed:

$\{\tilde{e}_1^l(t), \tilde{e}_2^l(t), \tilde{e}_3^l(t), \tilde{e}_4^l(t)\}$

4) For simplicity, pad each record $\{\tilde{e}_1^l(t), \tilde{e}_2^l(t), \tilde{e}_3^l(t), \tilde{e}_4^l(t)\}$ with a duration of T zeros at both the beginning and end, and compute the cross-correlation value for each receiver location as given by

$$C_i^{kl} = \frac{\max_{t \in (-T, 2T)} \left(\int_0^T e_i^k(\tau) \tilde{e}_i^l(t + \tau) d\tau \right)}{\left(\int_0^T (e_i^k(\tau))^2 d\tau \int_0^T (\tilde{e}_i^l(\tau))^2 d\tau \right)^{1/2}}. \quad (3)$$

5) Compute the stacked cross-correlation value by summing over all four receiver locations to obtain

$$C^{kl} = \frac{1}{4} \sum_{i=1}^4 C_i^{kl}. \quad (4)$$

The maximum value of C^{kl} occurs near time $t = 0$, and is recorded in the k^{th} row and l^{th} column in Table 1 below. Correlation values are highest when the location of the tensile crack and the location of the force impulse are the same.

Table 1 Stacked Cross-Correlation Values.

		Tensile Crack Source Location			
Force Impulse Source Location		S_1	S_2	S_3	S_4
	S_1	0.92	0.78	0.79	0.84
	S_2	0.78	0.92	0.84	0.79
	S_3	0.77	0.92	0.91	0.81
	S_4	0.88	0.77	0.81	0.91

5. CONCLUSIONS

By applying a time-reversed reciprocal method to a two-story one-bay steel frame, the location and application time of an impulse-like force can be determined.

The velocity waveform of a tensile crack can be approximated by the velocity waveform of an impulse-like force applied at the same beam-column connection of a steel frame.

The results support the use of waveform cross-correlation using a pre-event catalog of Green's function templates to determine the location and time of occurrence of a subsequent fracture recorded on a network of vibration sensors.

Acknowledgements:

The authors acknowledge support from the Hartley Foundation. The authors thank Brad Aagaard for the significant time and effort invested in making PyLith available.

References:

- Aagaard, B., Williams, C., and Knepley, M. (2008), "PyLith: A finite-element code for modeling quasi-static and dynamic crustal deformation," *Eos Transactions, Fall Meeting Supplement*, American Geophysical Union, **89**(53), Abstract T41A-192.
- Anstey, N.A. (1964) "Correlation Techniques – A Review," *Geophysical Prospecting*, **12**(4), 355-382.
- Clinton, J.F., Bradford, S.C., Heaton, T.H., and Favela, J. (2006) "The Observed Wander of the Natural Frequencies in a Structure," *Bulletin of the Seismological Society of America*, **96**(1), 237-257.
- Gibbons, S.J. and Ringdal, F. (2005), "The detection of low magnitude seismic events using array-based waveform correlation," *Geophysical Journal International*, **165**(1), 149-166.
- Giurgiutiu, V. and Cuc, A. (2005), "Embedded Non-destructive Evaluation for Structural Health Monitoring, Damage Detection, and Failure Prevention," *Shock and Vibration Digest*, **37**(2), 83-105.
- Kohler, M.D., Heaton, T.H., and Heckman V.M. (2009) "A Time-Reversed Reciprocal Method for Detecting High-Frequency Events in Civil Structures with Accelerometer Arrays," *Proceedings of the Fifth International Workshop on Advanced Smart Materials and Smart Structures Technology*.
- Park, H.W., Sohn, H., Law, K.H., and Farrar, C.R. (2007) "Time reversal active sensing for health monitoring of a composite plate," *Journal of Sound and Vibration* **302**(1-2), 50-66.
- Rodgers, J.E., Mahin, S.A., and Celebi, M. (2007) "Proposed Approaches to Fracture Damage Detection for Sparsely Instrumented Steel Moment-framed Buildings," *International Journal of Steel Structures*, **7**(1), 1-10.
- Wang, C.H., Rose, J.T., and Chang, F.K. (2004) "A synthetic time-reversal imaging method for structural health monitoring," *Smart Materials and Structures*, **13**(2), 415-423.
- Wang, C.H., and Rose, L.R.F. (2003) "Wave reflection and transmission in beams containing delamination and inhomogeneity," *Journal of Sound and Vibration*, **264**(4), 851-872.